JOC The Journal of Organic Chemistry

Article

pubs.acs.org/joc

Understanding the Effects of Preorganization, Rigidity, and Steric Interactions in Synthetic Barbiturate Receptors

Jacqueline M. McGrath and Michael D. Pluth*

Department of Chemistry and Biochemistry, Materials Science Institute, University of Oregon, Eugene, Oregon 97403-1253, United States

Supporting Information

ABSTRACT: Synthetic barbiturate receptors have been utilized for many applications due to their high binding affinities for complementary guests. Although interest in this class of receptors spans from supramolecular to materials chemistry, the effects of receptor steric bulk and preorganization on guest binding affinity has not been studied systematically. To investigate the roles that steric bulk and preorganization play in guest binding, we prepared a series of 12 deconstructed Hamilton receptors with varying degrees of steric bulk and preorganization. Both diethylbarbital and 3-methyl-7-propylxanthine were investigated as guests for the synthetic receptors. The stoichiometry of guest binding was investigated using Job plots for each host–guest pair, and ^{1}H NMR titrations were performed to measure the guest binding affinities. To complement the solution-state studies, DFT calculations at the B3LYP/6-31+G(d,p) level of theory employing the IEF-PCM $CHCl_3$ solvation model were also performed. Calculated guest binding energies correlated well with the experimental findings and provided additional insight into the factors influencing guest binding. Taken together, the results presented highlight the interplay between preorganization and steric interactions in establishing favorable interactions for self-assembled hydrogen-bonded systems.

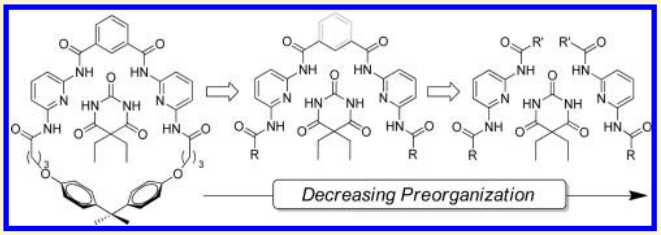

INTRODUCTION

Hydrogen-bonding interactions are a widely used structural arrangement found in many synthetic supramolecular structures. Although individual hydrogen bonds are much weaker than covalent bonds, hydrogen-bonding interactions commonly form cooperative networks when multiple donor and acceptor components combine. The fidelity of such networks can be maximized by encoding attractive primary and secondary interactions in the hydrogen-bonding structures[1,2] or by increasing the preorganization of hydrogen-bonding components to reduce the entropic cost for self-assembly.[3] Similarly, the reversibility of hydrogen-bond formation allows for errors in the assembly process to be repaired, leading to formation of the thermodynamically favored product. By engineering complementary hydrogen-bonding arrays into geometrically controlled molecular components, larger self-assembled structures, including foldamers, homo- and heteromultimeric structures, and cavity-containing 3D supramolecular host molecules, can be accessed.[4−15]

One such class of self-assembled hydrogen-bonded host–guest complexes are synthetic barbiturate receptors. Also known as Hamilton receptors, this well-studied class of macrocyclic synthetic receptors bind barbituric acid derivatives in complementary, preorganized hydrogen-bonding motifs (Figure 1).[16−21] Such receptors typically employ two hydrogen-bond donor–acceptor–donor (DAD) units that align with the two acceptor–donor–acceptor (ADA) faces of the barbiturate. The macrocyclic preorganization found in most prototypical synthetic barbiturate receptors results in high guest binding affinities typically ranging from 10^4 to 10^5 M^{-1}.[16,22] In addition to binding barbiturates, this class of receptors accommodates other guests with the appropriate complementary hydrogen-bonding arrays including uracils,[23−26] thymines,[23,24,26−30] succinimides,[24,31] glutarimides,[18,24,32] cyanuric acids,[23,33−35] and dipyridine-2-ylamines,[31,32] demonstrating the versatility of the receptor scaffolds. This diversity has resulted in the use of synthetic barbiturate receptors in different applications including catalysis,[36−38] electrooptical materials,[34,35,39] and supramolecular dendrimers.[33,40,41] Despite the prevalence of this receptor motif in various disciplines, the impacts of ligand preorganization, such as the importance of the macrocyclic effect or of ligand flexibility, remain unexplored.

Although nonmacrocyclic barbiturate receptors have been prepared, studies of such scaffolds have primarily focused on interactions in the solid state. For example, nonmacrocyclic barbiturate receptors have been thoroughly exploited in the solid state to bind nanoparticles to surfaces,[42−44] but the solution state binding behavior of these receptors has not been investigated comprehensively. Investigation of such systems could provide valuable insight into the interplay between steric interactions near the hydrogen-bonding moieties and the requirements of preorganization required for efficient guest binding.

Received: November 12, 2013

dx.doi.org/10.1021/jo402500a | J. Org. Chem. XXXX, XXX, XXX−XXX

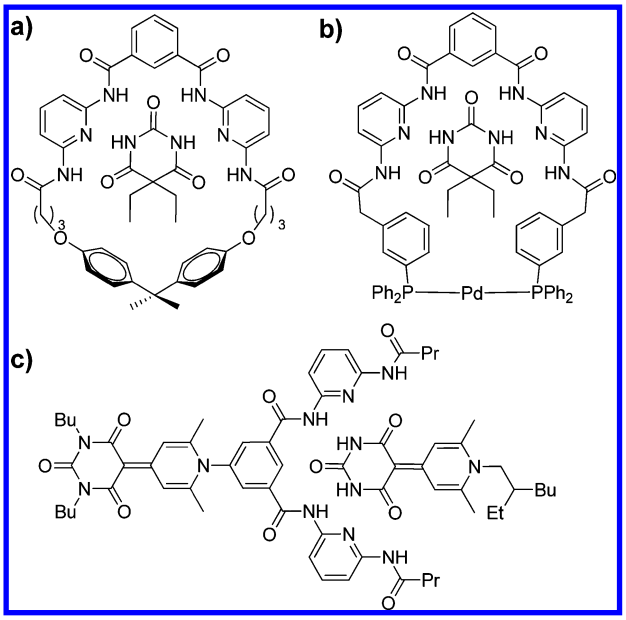

Figure 1. Selected examples of synthetic barbiturate receptors. (a) Prototypical Hamilton receptor; (b) chelating bis(phosphine) barbiturate receptor; and (c) highly conjugated nonmacrocyclic barbiturate receptor.

Toward our goal of understanding the assembly requirements of deconstructed supramolecular systems, and to probe the requirements of ligand rigidity, macrocylization, and preorganization on barbiturate receptor designs, we have systematically deconstructed barbiturate receptors into simple subunits to determine the effects of ligand bifurcation on barbiturate binding. By measuring the binding affinities and stoichiometries of both barbital and xanthine guests with rigid, flexible, or bifurcated ligands, we directly investigated the preorganization requirements for self-assembly. To complement the experimental results, we also screened and refined different DFT computational methods to generate a model that correlated well with solution data. Taken together, these results help to establish the requirements for effective barbiturate binding in synthetic host molecules and can be applied to other host–guest systems in which receptor preorganization is a requirement for self-assembly.

RESULTS AND DISCUSSION

To further understand the effect that preorganization and steric interactions play in determining the guest binding affinities of barbiturate receptors, we deconstructed prototypical macrocyclic barbiturate receptors into more simple subunits (Figure 2). The impacts of steric constraints on guest binding were investigated by preparing a library of symmetric (**1a–c**) or unsymmetric (**1d–f**) bifurcated hosts with methyl, phenyl, or *tert*-butyl groups on the peripheral amides. Similarly, the role of preorganization on self-assembly was investigated by preparing two receptor sets with either a flexible alkyl spacer between the two 2,6-dicarboxamido pyridine units (**3a–c**) or a rigid phenyl spacer between the 2,6-diamidopyridine units (**4a–c**). Both barbital (**5**) and 3-methyl-7-propylxanthine (**6**) were used as guests to investigate the structures and stoichiometries of the hydrogen-bonded constructs.

Synthesis. Symmetric 2,6-dicarboxamido pyridine hosts **1a–c** were prepared from 2,6-diaminopyridine by reaction with the desired acid chloride in the presence of triethylamine. To prepare unsymmetric 2,6-dicarboxamido pyridine receptors **1d–f**, 2,6-diaminopyridine was first reacted with 1 equiv of the desired acid chloride in the absence of base to afford monoamido pyridines **2a–c**, followed by installation of a second amide by treatment with a second acid chloride (Scheme 1). Nonmacrocyclic barbiturate receptors were

Scheme 1. Preparation of Hydrogen-Bonding Ligands Based on 2,6-Dicarboxyamido Pyridine Scaffolds

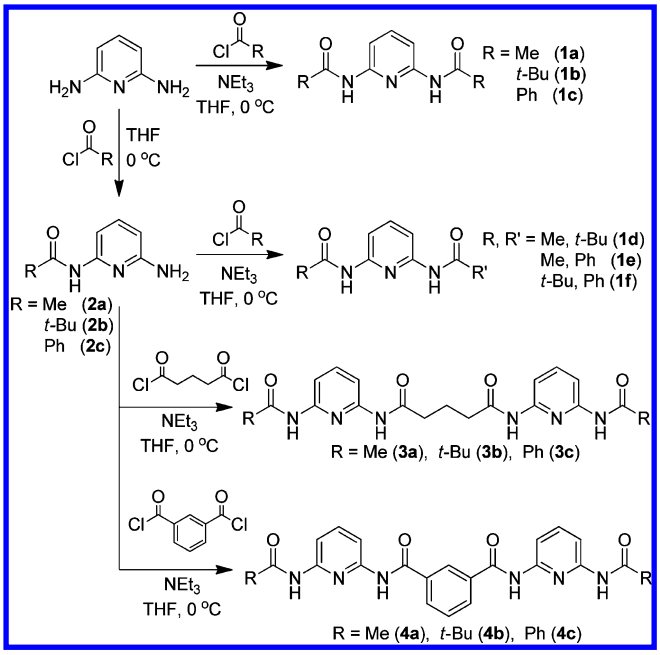

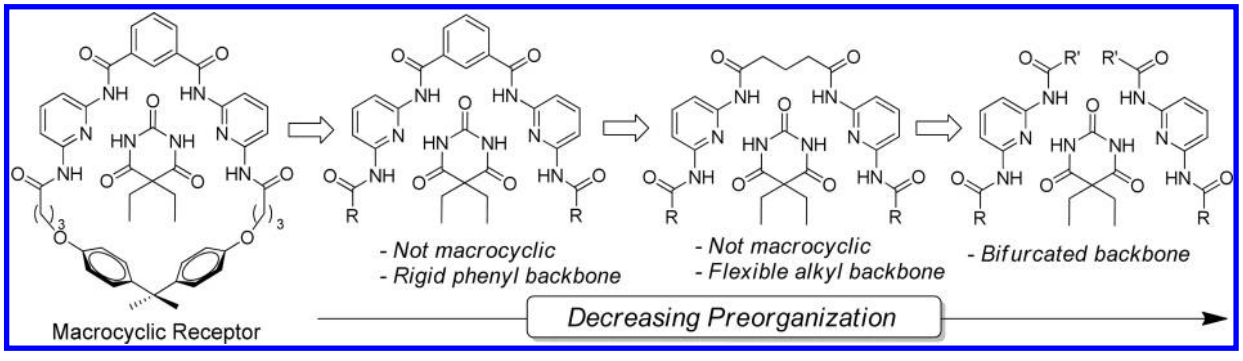

Figure 2. Deconstruction of Hamilton receptors to determine effects of preorganization and steric bulk.

dx.doi.org/10.1021/jo402500a | J. Org. Chem. XXXX, XXX, XXX–XXX

prepared with both flexible and rigid linkers between the two 2,6-dicarboxamido pyridine units. Treatment of glutaric acid with $SOCl_2$ afforded glutaryl chloride, which was treated with monoamines **2a–c** to afford the flexible barbiturate receptors **3a–c**. Similarly, treatment of isophthalic acid with $SOCl_2$ generated isophthalolyl chloride, which was treated with monoamines **2a–c** to generate rigid backbone ligands **4a–c**.

Host–Guest Binding Studies. To obtain binding constants for the deconstructed barbiturate receptors, ^{1}H NMR titrations were performed for each receptor/guest pair. Because guest binding involves hydrogen bonding of the amide N–H groups of both the host and the guest molecules, changes in N–H chemical shift reflect the position of the thermodynamic host–guest equilibrium during the course of the titration. To test the barbiturate binding affinity of each host construct, we used barbital (**5**) as the guest due to its high solubility and previous use as a guest in similar systems.[16,23] Barbital has two hydrogen-bonding ADA faces that can interact with the DAD faces of prototypical barbiturate receptors. For receptors with flexible (**3a–c**) or rigid (**4a–c**) backbones, **5** is expected to form a 1:1 host/guest complex with each face of **5** interacting with each DAD face of the ligand. For bifurcated ligands **1a–f**, either a 1:1 or a 2:1 host/guest complex could be formed, depending on the relative magnitude of the enthalpic gain upon hydrogen bonding and the entropic penalty for assembly of three components. In addition to using **5** as a guest, we also performed titrations with 3-methyl-7-propylxanthine (**6**), which has only one ADA face, thus simplifying the possible binding modes (Figure 3). Furthermore, **6** is less likely to self-

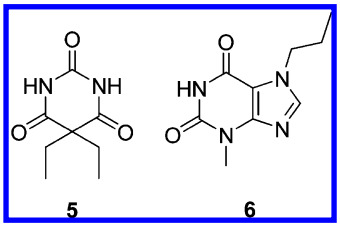

Figure 3. Barbital (**5**) and 3-methyl-7-propylxanthine (**6**) guests used in the titration studies with ligands **1a–f**, **3a–c**, and **4a–c**.

aggregate in solution, whereas barbital derivatives, such as **5**, are known to form self-complementary hydrogen-bonded oligomers.[45] Previous studies with similar host systems have shown negligible host dimerization.[23,32] For each host–guest system, a Job plot was constructed to determine the stoichiometry of guest binding. After establishing the binding stoichiometry, ^{1}H NMR titrations were performed in triplicate and the N–H chemical shifts of the guest were followed during the titrations. The resulting data were fit to the established binding stoichiometry.[46] Figure 4 shows the characteristic shift in the N–H ^{1}H NMR resonances used to quantify guest binding.

Job plots of bifurcated barbiturate receptors **1a–f** with **5** and **6** revealed 1:1 binding stoichiometries, suggesting that the entropic penalty to form the three-component system with **5** was too large for the relatively weak binding of **1a–f** with **5** and **6** to overcome. The binding affinities of 2,6-dicarboxamido pyridine hosts **1a–f** for guests **5** and **6** depended greatly on the steric bulk at the periphery of the receptor (Table 1). For example, replacing one or both methyl groups of **1a** with *tert*-butyl groups (**1d**, **1f**) reduces the binding affinities of **5** and **6** by almost 1 order of magnitude per *tert*-butyl group. This sizable reduction in binding affinity is likely due to the more twisted guest approach angle required to avoid disfavorable steric interactions between the host and the guest (*vide infra*). Similar trends are observed for the addition of phenyl groups, although the magnitude of the decrease in binding affinity is attenuated, which is likely due to rotation of the phenyl group away from the guest to minimize disfavored steric interactions. In all cases, binding constants for **6** were larger than those determined for **5**, which is consistent with the propensity of **5** to form hydrogen-bonded aggregates. Compared to binding affinities of macrocyclic receptors ($K_a \approx 10^4$ M^{-1}), these results demonstrate that complete bifurcation of Hamilton-derived receptors greatly diminishes guest binding affinity, thus suggesting that greater host preorganization is required to generate high-fidelity guest binding.

To further investigate the degree of preorganization required for optimal guest binding, receptors **3a–c** and **4a–c** were prepared. These scaffolds employ either flexible (**3a–c**) or rigid (**4a–c**) linkers in the backbone to allow for the degree of preorganization to be modified. Because both of the 2,6-dicarboxamido pyridine groups in these receptors are tethered together, the entropic penalty for binding **5** should be attenuated. By contrast, hosts **3a–c** and **4a–c** could potentially form either 1:1 or 1:2 host/guest complexes with **6** because **6** does not have entirely complementary interactions to interface with the two DAD faces of the receptor leaving one side of the receptor face free to interact with a second guest. For these receptors, increased steric bulk of the tethered host will reduce the overall binding affinity and more likely result in 1:1 complex formation due to the reduced capacity for multiple guests.

Consistent with the results obtained from bifurcated hosts **1a–f**, steric interactions from the receptor periphery greatly impacted guest binding for the scaffolds with flexible backbones **3a–c**. For example, replacing the methyl groups in **3a** with *tert*-butyl groups (**3b**) resulted in a 60-fold decrease in barbital binding. This observation is consistent with the bifurcated 2,6-dicarboxamido pyridine hosts (**1a–f**) and demonstrates the sensitivity to steric repulsion near the hydrogen-bonding sites. Flexible receptors **3a–c** also maintained higher binding affinity for **6** than for **5**, although the magnitude of this preference was diminished. Job plots of **3a–c** with **5** and **3b,c** with **6** confirmed 1:1 host/guest binding. Investigations of **3a** with **6**, however, revealed two binding events corresponding to the formation of 1:1 and 1:2 host/guest complexes. The first binding event, corresponding to a 1:1 **3a:6** complex, had a K_a of 1230 M^{-1}, which was one order of magnitude greater than binding of a second guest with a K_a of 180 M^{-1}. The difference in K_a values between the first and second guest binding events are consistent with the required elongation and corresponding entropic penalty of **3a** to accommodate two xanthine guests. Although 2:1 binding was observed with **6**, only 1:1 binding was observed with **5**. If barbital were to form a 1:2 host/guest complex, then the benefits from the chelate effect would need to be sacrificed in order to accommodate two barbital guests (Figure 5).

Job plots of **5** and **6** with **4a–c** confirmed exclusively 1:1 binding, and ^{1}H NMR titration data were subsequently fit to a 1:1 model. For **5**, the methyl end-capped host (**4a**) had the highest binding affinity, followed by the *tert*-butyl (**4b**) and finally the phenyl (**4c**) analog. Although phenyl groups are less sterically demanding than *tert*-butyl groups, the requirement of phenyl group rotation to accommodate a bound guest results in

dx.doi.org/10.1021/jo402500a | J. Org. Chem. XXXX, XXX, XXX–XXX

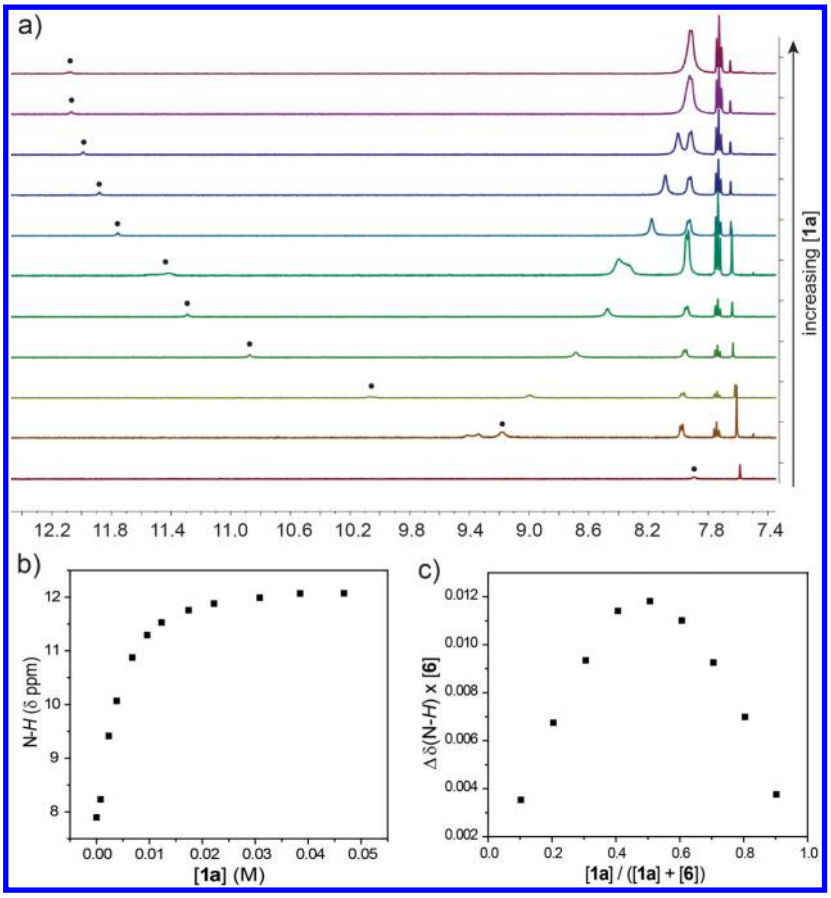

Figure 4. Representative ^{1}H NMR (500 MHz, 25 °C, $CDCl_3$) titration data for **1a** with **6**. (a) Stacked ^{1}H NMR titration spectra; (b) plot of the N-*H* chemical shift data from the ^{1}H NMR titration; and (c) Job plot for **1a** binding to **6** confirming a 1:1 binding stoichiometry.

Table 1. Binding Constants for 5 and 6 with Deconstructed Barbituric Acid Receptors 1a–f, 3a–c, and 4a–c[a]

	binding constant (K_a, M^{-1})			binding constant (K_a, M^{-1})	
	5	**6**		**5**	**6**
1a	85 ± 25	490 ± 70	**3a**	70 ± 37[b]	K_{a1} = 1230 ± 280[b] K_{a2} = 184 ± 78[b]
1b	2 ± 1	3 ± 1	**3b**	40 ± 4 –[b,c]	74 ± 15 7 ± 1[b]
1c	7 ± 2	21 ± 3	**3c**	–[b,c]	24 ± 7[b]
1d	17 ± 2	28 ± 2	**4a**	139 ± 18[b]	70 ± 9[b]
1e	29 ± 1	109 ± 14	**4b**	174 ± 3 6 ± 2[b]	40 ± 3 7 ± 5[b]
1f	3 ± 1	6 ± 1	**4c**	4 ± 8[b]	22 ± 10[b]

[a]Titrations were performed in $CDCl_3$ at 25 °C. All measurements are the average of at least three independent titrations. [b]Performed in 5% DMSO in $CDCl_3$ due to poor solubility of either the host or the host–guest complex. [c]Binding constant too low (<5 M^{-1}) to measure accurately.

a reduction of the conjugation into the amide and thereby reduces the enthalpic gain upon guest binding. As expected, the rigid backbone hosts had lower affinities for **6** than **5** due to constrained binding pockets present in the host constructs and greater steric bulk of **6** in comparison to **5**. Similar to trends observed for other host–guest pairs, steric bulk on the periphery of receptors **4a–c** directly affected the binding affinity toward **6**.[23,32]

The interplay between preorganization and steric interactions between host and guest is also observed across the different types of receptors. For example, by comparing the binding affinities of **5** with *tert*-butyl substituted receptors **1b**, **3b**, and **4b**, a clear trend is apparent, with the more preorganized structures producing stronger binding. Upon increasing the preorganization, the binding affinity for **5** increases from 2 M^{-1} for **1b**, to 40 M^{-1} for **3b**, and finally to 139 M^{-1} for **4b**. This series clearly demonstrates that host preorganization can offset some of the disfavorable steric interactions present in this series of receptors. A second trend is observed for the same series of host molecules interacting with **6**. In this case, because the xanthine guest cannot form favorable interactions with both sides of the symmetric receptors **3b** and **4b**, the steric influences are more important. The increase of binding affinities from 3 M^{-1} for **1b** to 75 M^{-1} for **3b** is primarily due to the decreased steric bulk from the flexible propyl chain by comparison to a *tert*-butyl group. Replacement of the flexible backbone of **3b** with the rigid phenyl backbone in **4b** slightly increases the steric encumbrance on the guest due to the inability of the phenyl group in **4b** to completely rotate away from the bound guest. As would be expected from these interactions, the binding constant of **6** with **4b** is lower than that for **3b**, but higher than that for **1b**. Taken together, these comparisons highlight the delicate balance between preorganization and minimization of steric interactions for synthetic barbiturate receptors.

To better understand the enthalpic and entropic effects associated with guest binding, we determined ΔH and ΔS using

dx.doi.org/10.1021/jo402500a | J. Org. Chem. XXXX, XXX, XXX–XXX

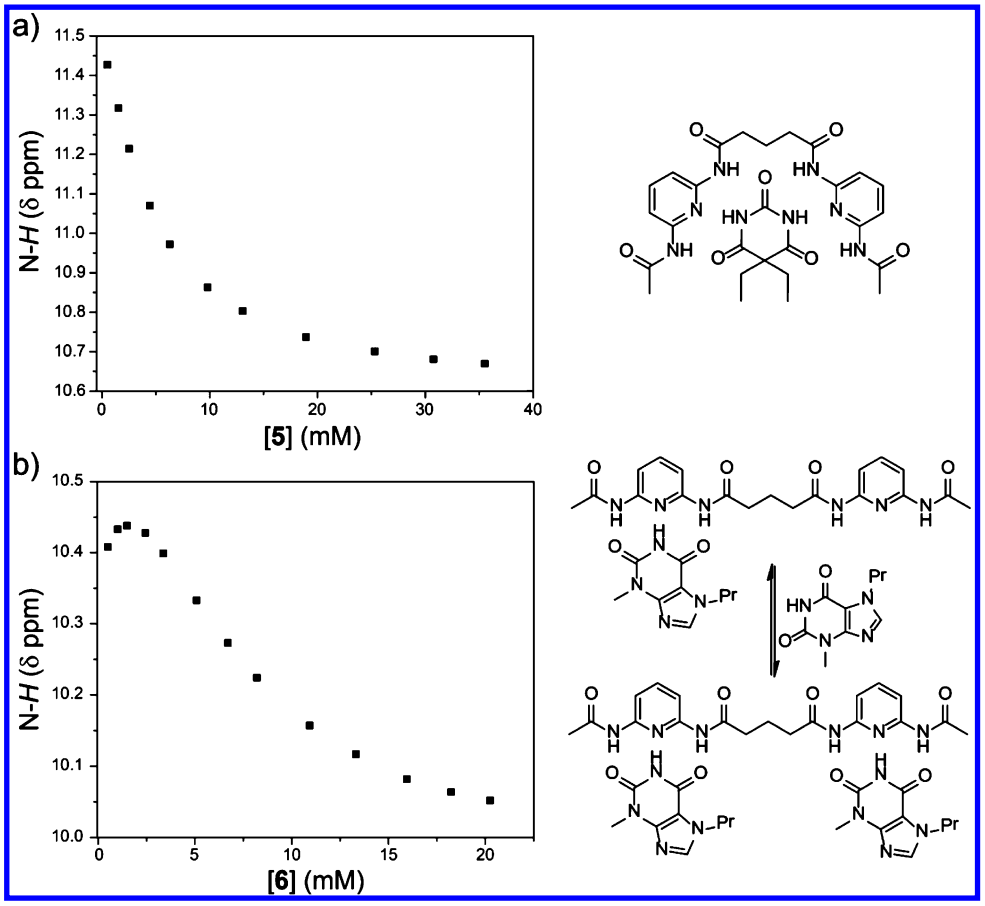

Figure 5. Representative ^{1}H NMR (500 MHz, 25 °C, 5% d_6-DMSO in $CDCl_3$) titration data for **1a** with **6**. Graph of the change in N−H chemical shift with changing concentrations of (a) **5** and (b) **6** in the presence of **3a**.

van't Hoff analysis for hosts **1a**, **1c**, and **1e** binding guest **6** (Figure S25). The binding enthalpies and entropies (ΔH, ΔS) were determined to be **1a** (−4.7 kcal/mol, −4.0 eu), **1c** (−3.8 kcal/mol, −6.5 eu), and **1e** (−5.8 kcal/mol, −10.1 eu). Both **1a** and **1c** have symmetric amide substituents, whereas **1e** does not. This desymmetrization results in preferential orientation of the guest to minimize the steric interaction between the propyl tail of **6** and the phenyl substituent of **1e**, resulting in a more negative binding entropy than was observed for **1a** or **1c**. Changes in the binding enthalpies are also observed. For example, **1c** has two phenyl substituents that must twist out of conjugation with the amide to allow for guest binding, which results in a lower observed binding enthalpy for **1c** by comparison to **1a** or **1e**.

Computational Studies on Hydrogen-Bonded Adducts. To gain further insight into the factors influencing host−guest binding, we optimized the structure of each host, guest, and hydrogen-bonded adduct using Gaussian 09 at the B3LYP/6-31+G(d,p) level of theory employing the IEF-PCM $CHCl_3$ solvation model. Based on the computed energies for each of the optimized geometries for each ligand, guest, and host−guest component, binding enthalpies were calculated (Table 2).[47] Although the DFT calculations overestimated the absolute magnitude of the binding energies, a good correlation between the experimentally determined binding affinities determined in $CDCl_3$ and the computed binding enthalpies was observed, suggesting that this computation level of theory can be used to reliably estimate trends in binding affinities of future similar barbiturate-binding scaffolds (Figure 6).

Table 2. Calculated Binding Energies for 5 and 6 with 1a−f, 3a−c, and 4a−c[a]

	$-\Delta H_{binding}$ (kcal/mol)			$-\Delta H_{binding}$ (kcal/mol)	
	5	**6**		**5**	**6**
1a	8.18	8.17	**3a**	10.88	9.40
1b	3.69	5.19	**3b**	5.18	7.41
1c	5.26	6.63	**3c**	3.98	8.53
1d	6.90	7.69	**4a**	12.69	8.13
1e	6.44	7.91	**4b**	7.96	8.17
1f	5.33	6.05	**4c**	10.83	6.96

[a]Calculated using Gaussian 09, B3LYP/6-31+G(d,p), with IEF-PCM solvation model for $CHCl_3$. Binding energies correspond to the difference in ZPE-corrected energies from the host−guest complexes and the isolated host and guest species.

Having established the validity of this computation model for estimating the magnitude of the binding interactions with the barbiturate-binding hosts, we used the optimized structures to gain insight into the major factors affecting guest binding affinities. By comparing the optimized geometries **1a−f** interacting with **5** and **6**, the steric bulk on the periphery of the receptors greatly affected the approach angle of **5** or **6** to the 2,6-dicarboxamido pyridine scaffolds. From comparison of the binding affinities of symmetric **1a−c** with **5**, **1a** forms the strongest interaction with **5** due to the limited repulsive steric interactions. The level of deviation from an ideal coplanar guest approach angle can be compared by measuring the angle between the least-squares planes of the pyridine ring of **1a** and

dx.doi.org/10.1021/jo402500a | J. Org. Chem. XXXX, XXX, XXX−XXX

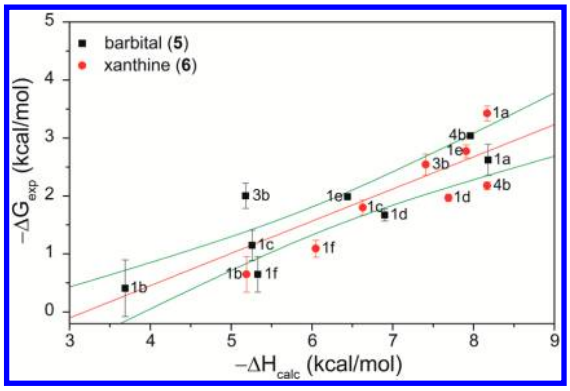

Figure 6. Comparison of experimentally determined binding affinities ($-\Delta G$, kcal/mol) with the calculated binding enthalpies, including linear fit (red) and 95% confidence interval (green).

the six-membered ring of **5**. From comparison of the guest approach angles with **5**, **1a** had the lowest approach angle of 15.1° angle, which increases to 32.3° for symmetric *tert*-butyl compound **1b**, and then decreased for the symmetric phenyl complex **1c** (Figure 7). These twist angles correlate strongly

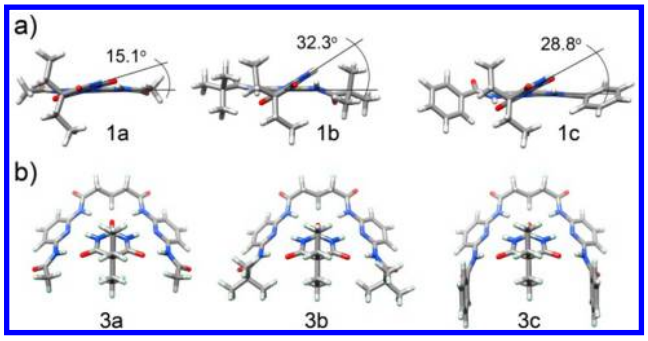

Figure 7. Examples of the optimized geometries for host−guest species **1a−c** with **5** (a) and **3a−c** with **5** (b). Changing the steric bulk of the periphery of the receptor influences the twist angel of the guest approach and the overall hydrogen-bonding fidelity.

with both the experimental and computational binding affinities. Similarly, for hosts tethered with either flexible or rigid backbones, the steric pressure exerted on the guest is greatly dictated by the size of the amide groups (Figure 7b). Although the phenyl groups can rotate to minimize steric interactions with the bound barbital, and potentially generate favorable CH−π interactions, this rotation results in a break of planarity with the amide, thereby reducing the overall conjugation of the system.

CONCLUSION

Both experimental titration data and DFT calculations show that both preorganization and steric bulk play a direct role in the binding affinity of the deconstructed Hamilton receptors. For the least preorganized hosts, **1a−f**, steric bulk had the largest role in influencing guest binding affinity with the least bulky host **1a** maintaining the highest binding affinities toward **5** and **6**, whereas the most bulky host, **1b**, had the smallest guest binding affinities. For hosts **3a−c** with moderate preorganization, the effects of steric bulk were attenuated. For the most rigid hosts, **4a−c**, steric interactions played a direct role in the guest binding affinities with the bulkiest host having the lowest affinity and the least bulky host having the highest binding affinity.

In addition to steric interactions, preorganization also played a distinct role in guest binding affinities. The more preorganized hosts, **4a−c**, had the highest binding affinity for barbital due to the high complementarity with the two hydrogen-bonding faces of **5**. The less preorganized hosts, **3a−c**, had higher binding affinities for **6** than did **4a−c** due to the flexibility of the ligand backbone, which allowed for two guests to be accommodated. The completely bifurcated hosts, **1a−f**, had much lower binding affinities than **3a−c** or **4a−c** due to the decreased ligand preorganization. Importantly, the combined experimental and computational results obtained for the deconstructed barbiturate receptors are also applicable to other hydrogen-bonding systems in which preorganization must be balanced with disfavorable steric interactions between the host and guest. These results illustrate the important roles that both sterics and preorganization play in host−guest complexes and how each should be either minimized or maximized in order to obtain the highest affinity for a given host−guest system.

EXPERIMENTAL SECTION

Materials and Methods. All commercially available reagents and deuterated solvents were used as received. Anhydrous solvents used for syntheses were collected from a solvent purification system. Reactions were monitored by TLC, and the products were purified on an automated flash chromatography instrument. NMR spectra were recorded at the indicated frequencies, and chemical shifts are reported in parts per million (δ) and are referenced to residual protic solvent resonances. The following abbreviations are used in describing NMR couplings: (s) singlet, (d) doublet, (t) triplet, (m) multiplet, and (b) broad.

General Job Plot Procedure. Job plots were performed in $CDCl_3$ and monitored by ^1H NMR for host molecules **1a−f**, **3b**, **3b**, and **4b**. Job plots with the host molecules **3a**, **3c**, **4a**, and **4c** were performed in 5% DMSO-d_6 in $CDCl_3$ due to poor solubility of the hosts in $CDCl_3$. All Job plots were performed using total (host + guest) concentrations of 10 mM, but compounds **1a−f** were also run at 100 mM total concentrations due to weaker guest binding. For a typical Job plot, 3 mL of a host solution and 3 mL of a guest solution were prepared and then divided between 10 NMR tubes in 10 mol % increments. After equilibration, the ^1H NMR spectrum for each sample was recorded and the shift in the guest N−H resonance was used to construct the Job plot.

General Procedure Binding Constant Determination. Binding studies were performed in $CDCl_3$ for host molecules **1a−f**, **3b**, and **4b** and monitored by ^1H NMR spectroscopy. Due to the poor solubility of compounds **3a**, **3c**, **4a**, and **4c** in $CDCl_3$, these compounds were measured in 5% DMSO-d_6 in $CDCl_3$. In order to compare the binding constants obtained in 5% DMSO-d_6 in $CDCl_3$ to those obtained in neat $CDCl_3$, titrations with host molecules **3b** and **4b** were also carried out in 5% DMSO-d_6 in $CDCl_3$. In a typical $CDCl_3$ titration, 2 mL of 1 mM **5** or **6** was prepared. The guest solution was then divided such that 1 mL was placed into an NMR tube and the other 1 mL was used to create a second solution containing 150−300 mM host. An initial spectrum of the guest was recorded, after which aliquots (5−100 μL) of the host solution were added until the N−H resonance of **5** or **6** no longer shifted. In a typical 5% DMSO-d_6 in $CDCl_3$ titration, 2 mL of a 3 mM host solution was prepared. The host solution was then divided such that 1 mL was placed into an NMR tube and the other 1 mL was used to create a second stock solution containing 25−100 mM guest. An initial spectrum of the host was recorded, after which aliquots (5−100 μL) of **5** or **6** were added until the N−H resonance of the **5** or **6** no longer shifted.

General van't Hoff Plot Procedure. Stock solutions of **1a**, **1c**, **1e**, and **6** were prepared at concentrations of 24, 120, 86, and 2 mM,

dx.doi.org/10.1021/jo402500a | J. Org. Chem. XXXX, XXX, XXX−XXX

respectively. These host concentrations were chosen to ensure complete host−guest complexation at the highest concentration. Six NMR samples of varying host/guest ratios were prepared for each host/guest pair, and the N−H resonance of **6** was monitored over the temperature range 298−328 K. All temperatures were calibrated using a MeOH temperature standard.[48]

Computational Details. Calculations were performed using the Gaussian 09[49] software package with the GaussView[50] graphical user interface. Graphical representations were produced using the UCSF Chimera package v1.8.[51] Initial conformational searches and optimizations were performed using either the 3-21g or 6-31g basis set, followed by full geometry optimizations and unscaled frequency calculations at the B3LYP/6-31+G(d,p) level of theory using the IEF-PCM solvation model for chloroform. Frequency calculations were performed on all converged structures confirming that they corresponded to local minima. Calculated enthalpies are reported as zero-point corrected enthalpies. In all cases, the lowest energy conformer was used to compare the relative energetics of the calculated species.

Syntheses. *N,N′-(Pyridine-2,6-diyl)diacetamide (**1a**).* A round-bottom flask was charged with dry THF (50 mL), 2,6-diaminopyridine (3.0 g, 28 mmol), and triethylamine (9.7 mL, 69 mmol). The flask was then lowered into an ice bath and degassed with N_2. Acetyl chloride (4.3 mL, 61 mmol) was added to an addition funnel containing dry THF (20 mL), and the resultant solution was then slowly added to the diaminopyridine solution while stirring in the ice bath under N_2. Once the addition of the acid chloride was complete, the ice bath was removed, and the reaction was allowed to warm to room temperature overnight while stirring under N_2. The reaction mixture was concentrated by rotary evaporation, and the crude product was purified by column chromatography (Si_2O, EtOAc) to afford **1a** as off-white crystals (5.2 g, 96% yield) with spectroscopic properties consistent with literature data.[32] Mp = 201−202 °C. ^{1}H NMR (500 MHz, $CDCl_3$) δ: 7.91 (d, J = 7.7 Hz, 2H), 7.73 (t, J = 7.9 Hz, 1H), 7.59 (s, 2H), 2.22 (s, 6H). $^{13}C\{^1H\}$ NMR (125 MHz, $CDCl_3$) δ: 168.5, 149.4, 140.9, 109.5, 24.8. HRMS (ESI-TOF) m/z: $[M + H]^+$ Calcd for $C_9H_{12}N_3O_2$, 194.0930; found 194.0932.

*N,N′-(Pyridine-2,6-diyl)dipivalamide (**1b**).* The monosubstituted diaminopyridine **2b** was prepared according to the general procedure outlined for **1a** with the following quantities: 2,6-diaminopyridine (33 mg, 0.30 mmol) in THF (15 mL) and trimethylacetyl chloride (81 μL, 0.66 mmol) in THF (15 mL). The crude product was purified by column chromatography (Si_2O, EtOAc) to afford a tan solid (83 mg, 99% yield) with spectroscopic properties consistent with literature data.[32] Mp = 112−113 °C. ^{1}H NMR (500 MHz, $CDCl_3$) δ: 7.94 (d, J = 7.8 Hz, 2H), 7.76 (s, 2H), 7.71 (t, J = 7.8 Hz, 1H), 1.34 (s, 18H) $^{13}C\{^1H\}$ NMR (125 MHz, $CDCl_3$) δ: 176.8, 149.6, 140.8, 109.3, 39.8, 27.5. HRMS (ESI-TOF) m/z: $[M + H]^+$ Calcd for $C_{15}H_{24}N_3O_2$, 278.1869; found 278.1859.

*N,N′-(Pyridine-2,6-diyl)dibenzamide (**1c**).* The monosubstituted diaminopyridine **1c** was prepared according to the general procedure outlined for **1a** with the following quantities: 2,6-diaminopyridine (31 mg, 0.28 mmol) in THF (15 mL) and benzoyl chloride (72 μL, 0.62 mmol) in THF (15 mL). The crude product was purified by chromatography (Si_2O, 1:1 EtOAc/DCM) to afford a tan solid (89 mg, 98% yield) with spectroscopic properties consistent with literature data.[52] Mp = 168−170 °C. ^{1}H NMR (500 MHz, $CDCl_3$) δ: 8.53 (s, 2H), 8.14 (d, J = 7.8 Hz, 2H), 7.93 (d, J = 7.3 Hz, 4H), 7.84 (t, J = 7.7 Hz, 1H), 7.60 (t, J = 7.3 Hz, 2H), 7.53 (t, J = 7.3 Hz, 4H). $^{13}C\{^1H\}$ NMR (125 MHz, $CDCl_3$) δ: 170.0, 165.5, 149.7, 141.3, 134.1, 133.6, 132.37, 130.0, 128.9, 128.5, 127.2, 110.01. HRMS (ESI-TOF) m/z: $[M + H]^+$ Calcd for $C_{19}H_{16}N_3O_2$, 318.1243; found 318.1247.

*N-(6-Acetamidopyridin-2-yl)pivalamide (**1d**).* A round-bottom flask was charged with dry THF (75 mL), **2a** (2.9 g, 19 mmol), and triethylamine (5.3 mL, 39 mmol). The flask was then lowered into an ice bath and degassed with N_2. Trimethylacetyl chloride (3.0 mL, 25 mmol) was added to an addition funnel containing dry THF (25 mL), and the resultant acid chloride solution was then slowly added to the diaminopyridine solution while stirring in the ice bath under N_2. Once the addition of the acid chloride was complete, the ice bath was removed and the reaction was allowed to warm to room temperature overnight while stirring under N_2. The reaction was concentrated by rotary evaporation, and the crude product was purified by column chromatography (SiO_2, EtOAc) to afford a white crystalline solid (3.88 g, 66%). Mp = 128−129 °C. ^{1}H NMR (500 MHz, $CDCl_3$) δ: 7.97 (d, J = 7.8 Hz, 1H), 7.91 (d, J = 7.5 Hz, 1H), 7.74 (m, 1H), 7.71 (s, 1H), 2.23 (s, 3H), 1.35 (s, 9H). $^{13}C\{^1H\}$ NMR (125 MHz, $CDCl_3$) δ: 176.9, 168.4, 149.7, 149.3, 140.9, 109.5, 109.3, 39.8, 27.5, 24.8. HRMS (ESI-TOF) m/z: $[M + H]^+$ Calcd for $C_{12}H_{18}N_3O_2$, 236.1399; found 236.1402.

*N-(6-Acetamidopyridin-2-yl)benzamide (**1e**).* The disubstituted diaminopyridine **1e** was prepared according to the general procedure outlined for **1d** with the following quantities: benzoyl chloride (1.9 mL, 16 mmol) in THF (25 mL) was added slowly to **2a** (1.9 g, 13 mmol) and triethylamine (3.6 mL, 26 mmol) in THF (50 mL). Purified by column chromatography (Si_2O, EtOAc) to afford a white crystalline solid (2.69 g, 81%). Mp = 195−196 °C. ^{1}H NMR (500 MHz, $CDCl_3$) δ: 8.34 (s, 1H), 8.10 (d, J = 7.8 Hz, 1H), 7.96 (d, J = 6.4 Hz, 1H), 7.92 (d, J = 7.8 Hz, 2H), 7.79 (m, 1H), 7.61 (t, J = 7.3 Hz, 1H), 7.53 (t, J = 8.3 Hz, 2H), 2.24 (s, 3H). $^{13}C\{^1H\}$ NMR (125 MHz, $CDCl_3$) δ: 165.4, 149.5, 140.0, 134.2, 132.3, 128.9, 127.1, 109.6, 24.8. HRMS (ESI-TOF) m/z: $[M + H]^+$ Calcd for $C_{14}H_{14}N_3O_2$, 256.1086; found 256.1097.

*N-(6-Pivalamidopyridin-2-yl)benzamide (**1f**).* The disubstituted diaminopyridine **1f** was prepared according to the general procedure outlined for **1d** with the following quantities: trimethylacetyl chloride (0.24 mL, 2.1 mmol) in THF (25 mL) was added slowly to **2c** (0.35 g, 1.6 mmol) and triethylamine (0.34 mL, 2.5 mmol) in THF (50 mL). Purified by column chromatography (Si_2O, CH_2Cl_2) to afford a chalky off-white solid (0.51 g, 82%). Mp = 120−121 °C. ^{1}H NMR (500 MHz, $CDCl_3$) δ: 8.33 (s, 1H), 8.06 (d, J = 8.3 Hz, 1H), 7.97 (d, J = 8.3 Hz, 1H), 7.94 (d, J = 4.3 Hz, 2H), 7.79 (s, 1H), 7.75 (t, J = 8.3, 1H), 7.56 (t, J = 7.3 Hz, 1H), 7.49 (t, J = 6.5 Hz, 2H), 1.32 (s, 9H). $^{13}C\{^1H\}$ NMR (125 MHz, $CDCl_3$) δ: 176.8, 165.4, 149.8, 149.6, 140.9, 134.2, 132.3, 128.9, 127.1, 109.7, 109.6, 39.8, 27.5. HRMS (ESI-TOF) m/z: $[M + H]^+$ Calcd for $C_{17}H_{20}N_3O_2$, 298.1556; found 298.1565.

*N-(6-Aminopyridin-2-yl)acetamide (**2a**).* A round-bottom flask was charged with dry THF (10 mL) and 2,6-diaminopyridine (1.0 g, 9.1 mmol). The flask was then lowered into an ice bath and degassed with N_2. Acetyl chloride (0.32 mL, 4.6 mmol) was added to an addition funnel containing dry THF (20 mL), and the resultant solution was then added slowly to the diaminopyridine solution over the course of 1 h while stirring at 0 °C under N_2. Once the addition of the acid chloride was complete, the ice bath was removed and the reaction was allowed to warm to room temperature overnight while stirring under N_2. The precipitate from the reaction was filtered, and the resultant filtrate was concentrated by rotary evaporation. The crude product was purified by column chromatography (SiO_2, EtOAc) to afford a tannish pink solid (0.65 g, 95%), with spectroscopic properties consistent with literature data.[32] Mp = 150−152 °C. ^{1}H NMR (300 MHz, $CDCl_3$) δ: 7.70 (s, 2H), 7.54−7.46 (m, 2H), 6.27 (d, J = 7.8 Hz, 1H), 4.32 (s, 2H), 2.18 (s, 3H). $^{13}C\{^1H\}$ NMR (125 MHz, $CDCl_3$) δ: 168.4, 157.0, 149.7, 140.2, 104.3, 103.3, 24.7. HRMS (ESI-TOF) m/z: $[M]^+$ Calcd for $C_7H_9N_3O$, 151.0746; found 151.0742.

*N-(6-Aminopyridin-2-yl)pivalamide (**2b**).* The monosubstituted diaminopyridine **2b** was prepared according to the general procedure outlined for **2a** with the following quantities: 2,6-diaminopyridine (0.51 g, 4.6 mmol) in THF (10 mL) and trimethylacetyl chloride (0.25 mL, 2.2 mmol) in THF (5 mL). Purified by column chromatography (Si_2O, EtOAc) to afford a tan solid (0.86 g, 97% yield), with spectroscopic properties consistent with literature data.[32] Mp = 131−132 °C. ^{1}H NMR (500 MHz, $CDCl_3$) δ: 7.73 (s, 1H), 7.59 (d, J = 8.3 Hz, 1H), 7.46 (t, J = 7.8 Hz, 1H), 6.26 (d, J = 7.81 Hz, 1H), 4.35 (s, 2H), 1.32 (s, 9H). $^{13}C\{^1H\}$ NMR (125 MHz, $CDCl_3$) δ: 168.3, 157.0, 149.8, 104.3, 103.3, 39.7, 27.5. HRMS (ESI-TOF) m/z: $[M + H]^+$ Calcd for $C_{10}H_{16}N_3O$, 194.1293; found 194.1295.

*N-(6-Aminopyridin-2-yl)benzamide (**2c**).* The monosubstituted diaminopyridine **2c** was prepared according to the general procedure outlined for **2a** with the following quantities: 2,6-diaminopyridine (2.0 g, 18 mmol) in THF (50 mL) and benzoyl chloride (1.0 mL, 9.0

dx.doi.org/10.1021/jo402500a | J. Org. Chem. XXXX, XXX, XXX−XXX

mmol) in THF (25 mL). Purified by column chromatography (Si_2O, CH_2Cl_2) to afford a white crystalline solid (3.53 g, 92%). Mp = 184−186 °C. ^{1}H NMR (500 MHz, $CDCl_3$) δ: 8.33 (s, 1H), 7.91 (d, J = 8.0 Hz, 2H), 7. 74 (d, J = 8.0 Hz, 1H), 7.59−7.50 (m, 4H), 6.32 (d, J = 8.0 Hz, 1H), 4.39 (s, 2H). ^{13}C{^{1}H} NMR (125 MHz, $CDCl_3$) δ: 165.4, 157.1,149.9, 104.3, 134.5, 132.1, 128.8, 127.1, 104.6, 103.5. HRMS (ESI-TOF) m/z: $[M + H]^+$ Calcd for $C_{12}H_{12}N_3O$, 214.0980; found 214.0974.

*N^1,N^5-Bis(6-acetamidopyridin-2-yl)glutaramide (**3a**).* Glutaric acid (0.21g, 1.6 mmol) was stirred in thionyl chloride (3 mL) for 5 h at room temperature, after which the thionyl chloride was removed under vacuum. A round-bottom flask was charged with dry THF (50 mL), **2a** (0.40 g, 2.7 mmol), and triethylamine (1.1 mL, 8.1 mmol). The flask was then lowered into an ice bath and degassed with N_2. The crude glutaroyl chloride was taken up in THF (10 mL) and added to an addition funnel. The resultant acid chloride solution was then slowly added to the diaminopyridine solution while stirring in the ice bath under N_2. Once the addition of the acid chloride was complete, the ice bath was removed and the reaction was allowed to warm to room temperature overnight while stirring under N_2. The reaction mixture was concentrated by rotary evaporation, and the residue was then taken up in EtOAc and washed with water and then saturated $NaHCO_3$. The organic layer was concentrated, and the resultant residue was then taken up in water (20 mL) and heated to 80 °C until all of the solid was dissolved. Upon cooling, the product crystallized as a white crystalline solid, which was collected by filtration and dried under vacuum (0.70 g, 65%). Mp = 221−222 °C. ^{1}H NMR (300 MHz, DMSO) δ: 10.52 (s, 2H), 10.19 (s, 2H), 8.54 (s, 2H), 8.18 (d, J = 7.3 Hz, 2H), 7.83 (s, 6H), 7.70 (t, J = 7.6 Hz), 3.36 (s, 4H), 2.14 (s, 2H). ^{13}C{^{1}H} NMR (125 MHz, DMSO) δ: 172.2, 169.7, 150.8, 143.3, 109.5, 35.8, 24.5, 21.1. HRMS (ESI-TOF) m/z: $[M + H]^+$ Calcd for $C_{19}H_{23}N_6O_4$, 399.1781; found 399.1799.

*N^1,N^5-Bis(6-pivalamidopyridin-2-yl)glutaramide (**3b**).* The alkyl tethered diaminopyridine **3b** was prepared according to the general procedure outlined for **3a** with the following quantities: glutaroyl dichloride (0.56 g, 3.3 mmol) in THF (20 mL) was added slowly to **2b** (1.1 g, 5.6 mmol) and TEA (1.4 mL, 10 mmol) in THF (50 mL). Purified by column chromatography (Si_2O, DCM with 5% of a 9:1 MeOH/NH_4OH mixture) to afford a white crystalline solid (1.11 g, 41%). Mp = 258 °C (dec). ^{1}H NMR (300 MHz, $CDCl_3$) δ: 7.95 (d, J = 8.1 Hz, 2H), 7.90 (s, 2H), 7.86 (d, J = 8.7 Hz, 2H), 7.77 (s, 2H), 7.71 (t, J = 8.1 Hz, 2H), 2.55 (t, J = 6.9 Hz, 4H), 2.16 (m, 2H), 1.33 (s, 18H). ^{13}C{^{1}H} NMR (125 MHz, $CDCl_3$) δ: 176.9, 170.7, 149.8, 149.2, 140.8, 109.6, 109.3, 39.8, 36.1, 27.5, 20.9. HRMS (ESI-TOF) m/z: $[M + H]^+$ Calcd for $C_{25}H_{35}N_6O_4$, 483.2720; found 483.2744.

*N^1,N^5-Bis(6-benzamidopyridin-2-yl)glutaramide (**3c**).* The alkyl tethered diaminopyridine **3c** was prepared according to the general procedure outlined for **3a** with the following quantities: glutaroyl dichloride (0.39 g, 2.3 mmol) in THF (20 mL) was added slowly to **2c** (0.81 g, 3.8 mmol) and TEA (1.6 mL, 11 mmol) in THF (50 mL). Purified by column chromatography (Si_2O, 3:2 hexanes/EtOAc) to afford a white crystalline solid (1.38 g, 67%). Mp = 179 °C (dec). ^{1}H NMR (500 MHz, $CDCl_3$) δ: 8.67 (s, 4H), 8.38 (d, J = 8.5 Hz, 2H), 7.84 (m, 6H), 7.50 (d, J = 8.0 Hz, 2H), 7.42 (t, J = 7.5 Hz, 4H), 6.89 (d, J = 8.0 Hz, 2H), 2.76 (t, J = 7.0 Hz, 4H), 2.08 (dd, J = 7.5, 8.0 Hz, 2H). ^{13}C{^{1}H} NMR (125 MHz, $CDCl_3$) δ: 173.0, 166.0, 152.0, 148.6,140.5, 134.2, 132.2, 128.6, 127.7, 119.7, 114.0, 32.3, 17.0. HRMS (ESI-TOF) m/z: $[M + H]^+$ Calcd for $C_{29}H_{27}N_6O_4$, 523.2094; found 523.2106.

*N^1,N^3-Bis(6-acetamidopyridin-2-yl)isophthalamide (**4a**).* Isophthalic acid (0.30 g, 1.8 mmol) was stirred in thionyl chloride (2 mL) at 65 °C with catalytic DMF for 7 h, after which the excess thionyl chloride was removed under vacuum. A round-bottom flask was charged with dry THF (50 mL), **2a** (0.44 g, 3.0 mmol), and triethylamine (1.2 mL 8.9 mmol). The flask was then lowered into an ice bath and degassed with N_2. The crude isophthaloyl chloride was taken up in dry THF (20 mL) and added to an addition funnel. The acid chloride solution was then slowly added to the diaminopyridine solution while stirring in the ice bath under N_2. Once the addition of the acid chloride was complete, the ice bath was removed and the reaction was allowed to warm to room temperature overnight while stirring under N_2. The reaction mixture was concentrated by rotary evaporation, and the residue was washed with water and then with saturated $NaHCO_3$. The organic layer was concentrated, and the resultant residue was then taken up in water (20 mL) and heated to 80 °C until all of the solid was dissolved. Upon cooling, the product crystallized as a white crystalline solid, which was collected by filtration and dried under vacuum (1.73 g, 45%). Mp = 161−163 °C. ^{1}H NMR (300 MHz, DMSO) δ: 10.51 (s, 2H), 10.18 (s, 2H), 8.53 (s, 1H), 8.16 (d, J = 7.3 Hz, 2H), 8.02 (d, J = 7.8 Hz, 2H), 7.92 (d, J = 7.3 Hz, 2H), 7.83 (m, 1H), 7.70 (t, J = 7.3 Hz, 2H), 2.17 (s, 6H). ^{13}C{^{1}H} NMR (125 MHz, DMSO) δ: 169.8 165.8, 151.1, 150.6, 140.5, 134.7, 161.8, 129.3, 127.9, 129.3, 127.9, 110.9, 110.3, 24.4. HRMS (ESI-TOF) m/z: $[M + H]^+$ Calcd for $C_{22}H_{21}N_6O_4$, 433.1624; found 433.1615.

*N^1,N^3-Bis(6-pivalamidopyridin-2-yl)isophthalamide (**4b**).* The alkyl tethered diaminopyridine **3e** was prepared according to the general procedure outlined for **3d** with the following quantities: isophthaloyl dichloride (1.0 g, 6.2 mmol) in THF (20 mL) was added slowly to **2b** (2.0 g, 10 mmol) and triethylamine (3.6 mL, 26 mmol) in THF (100 mL). Purified by column chromatography (Si_2O, 3:2 EtOAc/hexanes) to afford a white crystalline solid (2.89 g, 56%). Mp = 135−136 °C. ^{1}H NMR (500 MHz, $CDCl_3$) δ: 9.10 (s, 2H), 8.46 (s, 2H), 8.20−8.17 (m, 3H), 8.05 (d, J = 8.5 Hz, 2H), 7.97 (d, J = 8.0 Hz, 2H), 7.86 (t, J = 8 Hz, 2H), 7.72 (t, J = 8 Hz, 1H), 1.13 (s, 18H). ^{13}C{^{1}H} NMR (125 MHz, $CDCl_3$) δ: 177.0, 164.2, 149.9, 149.2, 141.0, 134.8, 130.8, 129.6, 125.8, 110.0, 109.0, 39.8, 27.5. HRMS (ESI-TOF) m/z: $[M + H]^+$ Calcd for $C_{28}H_{33}N_6O_4$ 517.2563; found 517.2574.

*N^1,N^3-Bis(6-benzamidopyridin-2-yl)isophthalamide (**4c**).* The alkyl tethered diaminopyridine **4c** was prepared according to the general procedure outlined for **3d** with the following quantities: isophthaloyl dichloride (0.23 g, 1.4 mmol) in THF (20 mL) was added slowly to **2c** (0.0.51 g, 2.4 mmol) and triethylamine (0.71 mL, 7.0 mmol) in THF (50 mL). Purified by column chromatography (Si_2O, 3:2 hexanes/EtOAc) to afford a white crystalline solid (0.88 g, 66%). Mp = 213−215 °C. ^{1}H NMR (300 MHz, $CDCl_3$) δ: 8.56 (s, 2H), 8.53 (s, 1H), 8.40 (s, 2H), 8.17 (d, J = 8.0 Hz, 4H), 8.14 (d, J = 8.0 Hz, 2H), 7.94 (d, J = 7.0 Hz, 4H), 7.87 (t, J = 8.0 Hz, 2H), 7.70 (t, J = 8.0 Hz, 1H), 7.61 (t, J = 7.5 Hz, 2H), 7.53 (t, J = 7.5 Hz, 4H). ^{13}C{^{1}H} NMR (125 MHz, $CDCl_3$) δ: 165.5, 164.2, 149.8, 149.4, 141.2, 134.8, 134.1, 132.4, 130.9, 128.9, 127.2, 110.3, 109.9. HRMS (ESI-TOF) m/z: $[M + H]^+$ Calcd for $C_{32}H_{25}N_6O_4$, 557.1937; found 557.1940.

■ ASSOCIATED CONTENT

Ⓢ Supporting Information

NMR spectra of new compounds, titration data, Job plots, van't Hoff plots, optimized geometries from DFT calculations. This material is available free of charge via the Internet at http://pubs.acs.org.

■ AUTHOR INFORMATION

Corresponding Author

*E-mail: pluth@uoregon.edu.

Notes

The authors declare no competing financial interest.

■ ACKNOWLEDGMENTS

We thank Mr. Ryan Hansen for assistance with preliminary titration data and Dr. Jesse Gavette for helpful discussions. This work was supported by funding from the University of Oregon. The NMR facilities at the UO are supported by the NSF/ARRA (CHE-0923589), and the computational infrastructure is supported by the OCI (OCI-096054). The Biomolecular Mass Spectrometry Core of the Environmental Health Sciences Core Center at Oregon State University is supported, in part, by the NIEHS (P30ES000210) and the NIH.

REFERENCES

(1) Sijbesma, R. P.; Meijer, E. W. *Chem. Commun.* **2003**, 5−16.
(2) Sontjens, S. H. M.; Meijer, J. T.; Kooijman, H.; Spek, A. L.; van Genderen, M. H. P.; Sijbesma, R. P.; Meijer, E. W. *Org. Lett.* **2001**, *3*, 3887−3889.
(3) Mardis, K. L. *J. Phys. Chem. B* **2006**, *110*, 971−975.
(4) Beijer, F. H.; Kooijman, H.; Spek, A. L.; Sijbesma, R. P.; Meijer, E. W. *Angew. Chem., Int. Ed.* **1998**, *37*, 75−78.
(5) Prins, L. J.; Reinhoudt, D. N.; Timmerman, P. *Angew. Chem., Int. Ed.* **2001**, *40*, 2382−2426.
(6) Whitesides, G. M.; Simanek, E. E.; Mathias, J. P.; Seto, C. T.; Chin, D. N.; Mammen, M.; Gordon, D. M. *Acc. Chem. Res.* **1995**, *28*, 37−44.
(7) ten Cate, A. T.; Sijbesma, R. P. *Macromol. Rapid Commun.* **2002**, *23*, 1094−1112.
(8) Schmuck, C.; Wienand, W. *Angew. Chem., Int. Ed.* **2001**, *40*, 4363−4364.
(9) Desiraju, G. R. *Acc. Chem. Res.* **1996**, *29*, 441−449.
(10) Armstrong, G.; Buggy, M. *J. Mater. Sci.* **2005**, *40*, 547−559.
(11) Adriaenssens, L.; Ballester, P. *Chem. Soc. Rev.* **2013**, *42*, 3261−3277.
(12) Rebek, J. *Chem. Soc. Rev.* **1996**, *25*, 255−264.
(13) Sijbesma, R. P.; Meijer, E. W. *Curr. Opin. Colloid Interface Sci.* **1999**, *4*, 24−32.
(14) Jasat, A.; Sherman, J. C. *Chem. Rev.* **1999**, *99*, 931−967.
(15) Price, S. L. *CrystEngComm* **2004**, *6*, 344−353.
(16) Chang, S. K.; Hamilton, A. D. *J. Am. Chem. Soc.* **1988**, *110*, 1318−1319.
(17) Berl, V.; Huc, I.; Lehn, J. M.; DeCian, A.; Fischer, J. *Eur. J. Org. Chem.* **1999**, 3089−3094.
(18) Chang, S. K.; Vanengen, D.; Fan, E.; Hamilton, A. D. *J. Am. Chem. Soc.* **1991**, *113*, 7640−7645.
(19) Collinson, S. R.; Gelbrich, T.; Hursthouse, M. B.; Tucker, J. H. R. *Chem. Commun.* **2001**, 555−556.
(20) Shivanyuk, A. N.; Rudkevich, D. M.; Reinhoudt, D. N. *Tetrahedron Lett.* **1996**, *37*, 9341−9344.
(21) Tecilla, P.; Jubian, V.; Hamilton, A. D. *Tetrahedron* **1995**, *51*, 435−448.
(22) Schmidt, J.; Schmidt, R.; Wurthner, F. *J. Org. Chem.* **2008**, *73*, 6355−6362.
(23) Beijer, F. H.; Sijbesma, R. P.; Vekemans, J.; Meijer, E. W.; Kooijman, H.; Spek, A. L. *J. Org. Chem.* **1996**, *61*, 6371−6380.
(24) Feibush, B.; Figueroa, A.; Charles, R.; Onan, K. D.; Feibush, P.; Karger, B. L. *J. Am. Chem. Soc.* **1986**, *108*, 3310−3318.
(25) Kotera, M.; Lehn, J. M.; Vigneron, J. P. *J. Chem. Soc., Chem. Commun.* **1994**, 197−199.
(26) Brienne, M. J.; Gabard, J.; Lehn, J. M.; Stibor, I. *J. Chem. Soc., Chem. Commun.* **1989**, 1868−1870.
(27) Yu, L. H.; Schneider, H. J. *Eur. J. Org. Chem.* **1999**, 1619−1625.
(28) Muehldorf, A. V.; Vanengen, D.; Warner, J. C.; Hamilton, A. D. *J. Am. Chem. Soc.* **1988**, *110*, 6561−6562.
(29) Hamilton, A. D.; Little, D. *J. Chem. Soc., Chem. Commun.* **1990**, 297−300.
(30) Goodman, M. S.; Rose, S. D. *J. Am. Chem. Soc.* **1991**, *113*, 9380−9382.
(31) Osmialowski, B.; Kolehmainen, E.; Gawinecki, R.; Kauppinen, R.; Koivukorpi, J.; Valkonen, A. *Struct. Chem.* **2010**, *21*, 1061−1067.
(32) Osmialowski, B.; Kolehmainen, E.; Gawinecki, R.; Dobosz, R.; Kauppinen, R. *J. Phys. Chem. A* **2010**, *114*, 12881−12887.
(33) Eckelmann, J.; Dethlefs, C.; Brammer, S.; Dogan, A.; Uphoff, A.; Luning, U. *Chem.—Eur. J.* **2012**, *18*, 8498−8507.
(34) Gnichwitz, J. F.; Wielopolski, M.; Hartnagel, K.; Hartnagel, U.; Guldi, D. M.; Hirsch, A. *J. Am. Chem. Soc.* **2008**, *130*, 8491−8501.
(35) Wessendorf, F.; Grimm, B.; Guldi, D. M.; Hirsch, A. *J. Am. Chem. Soc.* **2010**, *132*, 10786−10795.
(36) Larsen, J.; Rasmussen, B. S.; Hazell, R. G.; Skrydstrup, T. *Chem. Commun.* **2004**, 202−203.
(37) Sorensen, H. S.; Larsen, J.; Rasmussen, B. S.; Laursen, B.; Hansen, S. G.; Skrydstrup, T.; Amatore, C.; Jutand, A. *Organometallics* **2002**, *21*, 5243−5253.
(38) Li, Y.; He, Y. M.; Li, Z. W.; Zhang, F.; Fan, Q. H. *Org. Biomol. Chem.* **2009**, *7*, 1890−1895.
(39) Wurthner, F.; Schmidt, J.; Stolte, M.; Wortmann, R. *Angew. Chem., Int. Ed.* **2006**, *45*, 3842−3846.
(40) Grimm, F.; Hartnagel, K.; Wessendorf, F.; Hirsch, A. *Chem. Commun.* **2009**, 1331−1333.
(41) Dirksen, A.; Hahn, U.; Schwanke, F.; Nieger, M.; Reek, J. N. H.; Vogtle, F.; De Cola, L. *Chem.—Eur. J.* **2004**, *10*, 2036−2047.
(42) Binder, W. H.; Kluger, C.; Straif, C. J.; Friedbacher, G. *Macromolecules* **2005**, *38*, 9405−9410.
(43) Binder, W. H.; Kluger, C.; Josipovic, M.; Straif, C. J.; Friedbacher, G. *Macromolecules* **2006**, *39*, 8092−8101.
(44) Binder, W. H.; Lomoschitz, M.; Sachsenhofer, R.; Friedbacher, G. *J. Nanomater.* **2009**, 613813.
(45) Bolton, W. *Acta Crystallogr.* **1962**, *16*, 166−173.
(46) Thordarson, P. *Chem. Soc. Rev.* **2011**, *40*, 1305−1323.
(47) We also optimized and calculated binding enthalpies for the 2:1 barbital/2,6-biscarboxamido pyridine scaffolds even though we did not observe formation of these in solution, with the exception of **1a**. The binding affinity of the second 2,6-biscarboxamido pyridine ligand was slightly lower than the first, and the entropic penalty required for forming the 2:1 adducts may explain the lack of observation in solution. See the Supporting Information for tabulated 2:1 binding enthalpies.
(48) Findeisen, M.; Brand, T.; Berger, S. *Magn. Reson. Chem.* **2007**, *45*, 175−178.
(49) Frisch, M. J.; Trucks, G. W.; Schlegel, H. B.; Scuseria, G. E.; Robb, M. A.; Cheeseman, J. R.; Scalmani, G.; Barone, V.; Mennucci, B.; Petersson, G. A.; Nakatsuji, H.; Caricato, M.; Li, X.; Hratchian, H. P.; Izmaylov, A. F.; Bloino, J.; Zheng, G.; Sonnenberg, J. L.; Hada, M.; Ehara, M.; Toyota, K.; Fukuda, R.; Hasegawa, J.; Ishida, M.; Nakajima, T.; Honda, Y.; Kitao, O.; Nakai, H.; Vreven, T.; Montgomery, J. A., Jr.; Peralta, J. E.; Ogliaro, F.; Bearpark, M.; Heyd, J. J.; Brothers, E.; Kudin, K. N.; Staroverov, V. N.; Kobayashi, R.; Normand, J.; Raghavachari, K.; Rendell, A.; Burant, J. C.; Iyengar, S. S.; Tomasi, J.; Cossi, M.; Rega, N.; Millam, J. M.; Klene, M.; Knox, J. E.; Cross, J. B.; Bakken, V.; Adamo, C.; Jaramillo, J.; Gomperts, R.; Stratmann, R. E.; Yazyev, O.; Austin, A. J.; Cammi, R.; Pomelli, C.; Ochterski, J. W.; Martin, R. L.; Morokuma, K.; Zakrzewski, V. G.; Voth, G. A.; Salvador, P.; Dannenberg, J. J.; Dapprich, S.; Daniels, A. D.; Farkas, Ö.; Foresman, J. B.; Ortiz, J. V.; Cioslowski, J.; Fox, D. J. *Gaussian 09*, revision C.01; Gaussian, Inc., Wallingford, CT, 2009.
(50) Dennington, R.; Keith, T.; Millam, J. *GaussView*, version 5; Semichem Inc.: Shawnee Mission, KS, 2009.
(51) Pettersen, E. F.; Goddard, T. D.; Huang, C. C.; Couch, G. S.; Greenblatt, D. M.; Meng, E. C.; Ferrin, T. E. *J. Comput. Chem.* **2004**, *25*, 1605−1612.
(52) Langer, P.; Amiri, S.; Bodtke, A.; Saleh, N. N. R.; Weisz, K.; Gorls, H.; Schreiner, P. R. *J. Org. Chem.* **2008**, *73*, 5048−5063.